sustainability

MDPI

Article

The Côte d'Argent, France: Quantification of Plastic Pollution in Beach Sediments

Daniela Bornstein [1,†] **and Johannes Steinhaus** [1,2,*,†]

[1] Department of Natural Sciences, Bonn-Rhein-Sieg University of Applied Sciences, Von-Liebig-Straße 20, 53359 Rheinbach, Germany; daniela.bornstein@h-brs.de
[2] Institute of Technology, Ressource and Energy-Efficient Engineering (TREE), Grantham-Allee 20, 53757 Sankt Augustin, Germany
* Correspondence: johannes.steinhaus@h-brs.de; Tel.: +49-2241-865-458
† These authors contributed equally to this work.

Abstract: Pollution with anthropogenic waste, particularly persistent plastic, has now reached every remote corner of the world. The French Atlantic coast, given its extensive coastline, is particularly affected. To gain an overview of current plastic pollution, this study examined a stretch of 250 km along the Silver Coast of France. Sampling was conducted at a total of 14 beach sections, each with five sampling sites in a transect. At each collection site, a square of 0.25 m^2 was marked. The top 5 cm of beach sediment was collected and sieved on-site using an analysis sieve (mesh size 1 mm), resulting in a total of approximately 0.8 m^3 of sediment, corresponding to a total weight of 1300 kg of examined beach sediment. A total of 1972 plastic particles were extracted and analysed using infrared spectroscopy, corresponding to 1.5 particles kg^{-1} of beach sediment. Pellets (885 particles), polyethylene as the polymer type (1349 particles), and particles in the size range of microplastics (943 particles) were most frequently found. The significant pollution by pellets suggests that the spread of plastic waste is not primarily attributable to tourism (in February/March 2023). The substantial accumulation of meso- and macro-waste (with 863 and 166 particles) also indicates that research focusing on microplastics should be expanded to include these size categories, as microplastics can develop from them over time.

Keywords: Atlantic coast; microplastic; plastic pollution; beaching; infrared spectroscopy

Citation: Bornstein, D.; Steinhaus, J. The Côte d'Argent, France: Quantification of Plastic Pollution in Beach Sediments. *Sustainability* **2024**, *16*, 2992. https://doi.org/10.3390/su16072992

Academic Editors: Lord Abbey and Chijioke Emenike

Received: 20 February 2024
Revised: 22 March 2024
Accepted: 26 March 2024
Published: 3 April 2024

1. Introduction

Plastic is an essential, often indispensable, and ubiquitous material [1]. In the last decade, plastics, and especially plastic waste, have become the focus of interest at various societal and political levels [1,2]. The United Nations Environment Programme estimates that between 75 Mt to 199 Mt of plastic waste has accumulated in the oceans [3,4]. The uncontrolled disposal of waste on land, as well as waste production through fisheries and shipping, coupled with widespread single-use plastic consumption, has led to the accumulation of plastic waste in the environment [5]. Improperly disposed plastic waste not only impacts the environment but also coastal tourism; the disposal of plastic waste significantly increases costs for coastal communities (estimated at USD 197 billion in 2030) [5]. Without intervention, the amount of plastic waste entering aquatic ecosystems, which is currently around 1.7 Mt [6], is projected to increase to approximately 23 Mt to 37 Mt per year by 2040 [3–5]. The entry of plastic waste into the oceans is exclusively anthropogenic and can occur through various pathways [7,8]. Plastic waste varies in terms of plastic type, density, color, shape, and size. Once plastics enter the seas, they undergo decomposition and fragmentation due to sunlight, wind, water, mechanical abrasion, and other environmental influences [9–11]. A consistent definition of micro-, meso-, and macroplastics, particularly in terms of size, is currently lacking [1,7,9]. In many publications, including this one, microplastics are defined as particles with a size or length ranging from 1 µm to

5 mm. Mesoplastics are often defined as ranging from 5 mm to 25 mm, and macroplastics from 25 mm to 1 m [12]. Microplastics are further categorised into three types (see Figure 1): primary microplastics, intentionally manufactured within the specified size range [2,7]; primary unintentional microplastics, which result from the usage of macroplastics and subsequently break down into microplastics; and secondary microplastics, which result from the fragmentation of macro- and mesoplastics in the environment [8,13,14].

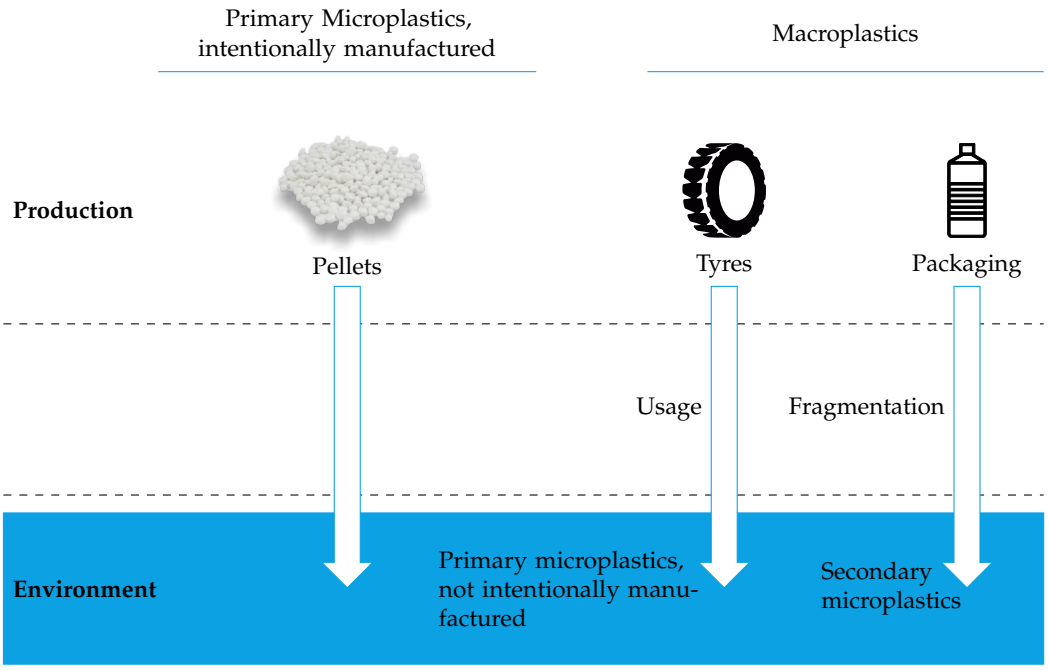

Figure 1. Schematic progression from the production of plastic to its distribution in the environment and transformation into microplastics (adapted from [15]).

As macro- and mesoplastics often serve as the origin of microplastics, it is crucial to systematically examine and analyze the transport and fate of these size groups in the environment [1,16]. Furthermore, the European Union (EU) directive 2008/56/EC of the European Parliament and Council, dated 17 June 2008, calls for the documentation of state descriptions regarding chemicals, sediment contamination, and pollution hotspots [17]. To enhance the understanding of the processes related to the accumulation of plastic waste in the environment and to assess the risk of plastic pollution, comprehensive environmental samples are important [1,18]. The number of studies on meso- and macroplastics is significantly lower than the number of studies on microplastics in the marine environment. In the studies used here from 2021 onward, it is evident that there is a research gap concerning these sizes, with 22 studies on microplastics [1,4,7,8,10,11,19–34] and 5 studies that include meso- and macroplastics [5,12,13,35,36]. Therefore, this study not only focuses on microplastics but also considers meso- and macroplastics, capturing particles ranging in size from 1 mm to 1000 mm. Attenuated Total Reflectance-Fourier Transform Infrared Spectroscopy (ATR-FTIR spectroscopy) is employed for detection, which is already an established standard method used in microplastic analysis. Due to the lack of studies, an assessment of current plastic pollution on the beaches along the entire French Silver Coast, the Côte d'Argent, was conducted [33,37,38]. In particular, the examination focused on the various sizes of micro-, meso-, and macroplastics; their distribution; as well as the type of plastic, their shape, and their existing color. This provides a comprehensive overview of plastic pollution.

2. Materials and Methods

2.1. Studied Area

The French Atlantic coast spans over 1200 km from Brittany in the north to the Spanish border in the south [39]. It has been heavily polluted with plastic waste for many decades. Particularly during winter when the sea is turbulent, a significant amount of debris is washed ashore [40]. The stormy season in the Bay of Biscay in the Golfe de Gascogne occurs between October and February [41]. The Côte d'Argent is situated in the southern part of the Golfe de Gascogne and features a predominantly sandy, straight coastline stretching approximately 250 km [33,39]. Figure 2 depicts the Côte d'Argent along with the respective sampling locations. Identifiers have been assigned to the beach names for convenience. Table 1 summarizes the beach names, their coordinates, and their associated identifiers.

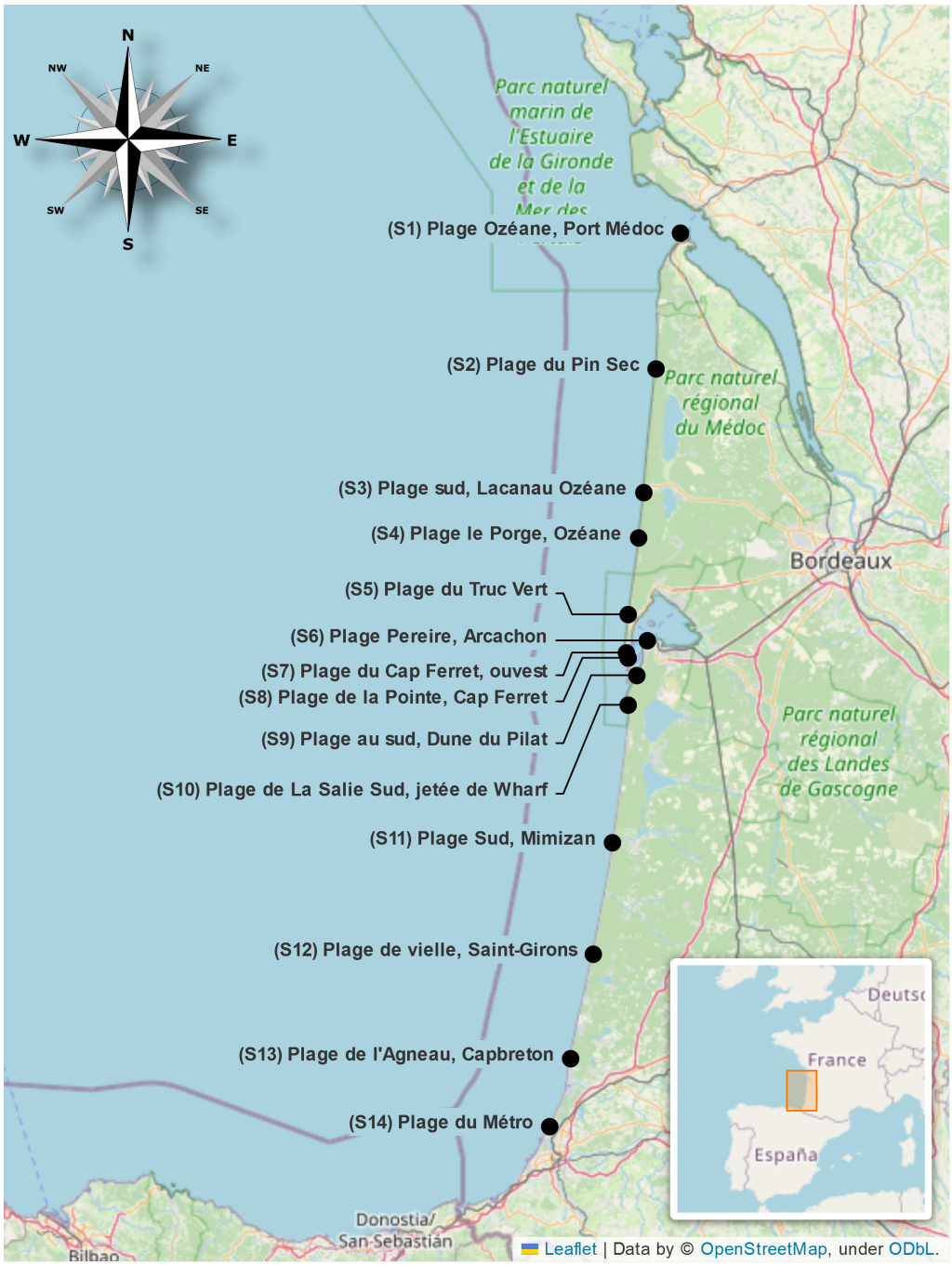

Figure 2. Map of the Côte d'Argent, marking the sampling locations (created with folium [42]).

Table 1. Sampling locations along the Côte d'Argent. Each sampling location is given an identifier (refer to Figure 2).

Beach Name	Coordinates		Identifier
Plage Ozéane, Port Médoc	43°33′33″ N	1°30′1″ W	S1
Plage du Pin Sec	43°42′50″ N	1°26′6″ W	S2
Plage sud, Lacanau Ozéane	43°57′14″ N	1°21′50″ W	S3
Plage le Porge, Ozéane	44°12′15″ N	1°18′1″ W	S4
Plage du Truc Vert	44°30′55″ N	1°15′16″ W	S5
Plage Pereire, Arcachon	44°34′53″ N	1°13′21″ W	S6
Plage du Cap Ferret, ouvest	44°37′21″ N	1°15′11″ W	S7
Plage de la Pointe, Cap Ferret	44°37′55″ N	1°15′33″ W	S8
Plage au sud, Dune du Pilat	44°39′33″ N	1°11′40″ W	S9
Plage de La Salie Sud, jetée de Wharf	44°43′3.4″ N	1°15′1.2″ W	S10
Plage Sud, Mimizan	44°53′30″ N	1°13′6″ W	S11
Plage de vielle, Saint-Girons	44°59′32″ N	1°12′11″ W	S12
Plage de l' Agneau, Capbreton	45°16′5″ N	1°9′59″ W	S13
Plage du Métro	45°33′60″ N	1°5′21″ W	S14

The Côte d'Argent is subject to numerous anthropogenic influences. In addition to intense touristic use of the beaches with approximately one million visitors per year, the coast is utilised for professional and recreational fishing, aquaculture, and recreational sports activities [33]. Furthermore, in the vicinity of the Bassin d'Arcachon, there is a wastewater system that transports industrial and municipal effluents from five different treatment plants (S10) [7,33].

2.2. Sampling

As part of this study, samples were collected from mid-February to mid-March 2023 along a 250 km stretch, as depicted in Figure 2. The selection of this season, situated between the winter and tourist seasons, was based on the reduced quantity of marine debris due to the calmer weather conditions, which also resulted in fewer disturbances during sample collection. Simultaneously, the tourist season was yet to commence, mitigating significant impacts on the discovered plastic waste. Additionally, outside of the peak season, there is a decrease in beach cleaning activities conducted by local municipalities. The beaches are exposed to waves and exhibit a meso-macrotidal regime [33,43]. Sampling was conducted on the beach section from Plage Océane Port Médoc to Plage du Métro, including sampling at the Bassin d'Arcachon and Dune du Pilat. A high tide line was consistently chosen for sampling. As standardized sampling strategies have not yet been established, various publications were consulted for guidance [16,37,44]. Sampling was conducted along a total of 14 beach sections, each with five sampling sites arranged in a transect [45]. The positioning of sampling sites along individual beach sections was determined before each sampling event by assessing the location of the high tide line. Additionally, the starting and ending points of each transect were identified before sampling commenced, and Global Positioning System (GPS) coordinates were recorded. Each transect spanned 100 m and ran parallel to the high tide line [16,46]. A sample was collected every 25 m, marked by a 0.25 m^2 square at each sampling site. The top 5 cm of sand was collected using a metal shovel. The sample was sieved on-site with a stainless steel analysis sieve (mesh size 1 mm) to minimize the transported sample volume. Due to challenges in sieving wet and highly clumping sand, a smaller mesh size could not be used. Therefore, 1 mm represents the lower limit of detectable particles. After sieving, all suspected plastic particles were collected using stainless steel tweezers and transferred to Petri dishes.

2.3. Preparation of Samples

The Petri dishes were opened and placed in a closed container with filtered warm air for drying. Subsequently, the samples were brushed with a natural bristle brush to remove

any remaining sand and organic material. Afterward, the Petri dishes were tightly sealed and stored in a cool environment until analysis.

2.4. Contamination Control

Precautions were taken from on-site sampling to chemical analysis in the laboratory to minimize sample contamination. Nitrile or cotton gloves were used during sample collection, and cotton lab coats along with nitrile gloves were used during laboratory analysis. Throughout the sampling process, the sample collectors positioned themselves leeward to avoid contamination from clothing. All materials and equipment used for sample preparation were washed with filtered ethanol and water. Due to the lower detection limit of 1 mm, significant cross-contamination was not expected.

2.5. Visual Sorting

The visual sorting of microplastic particles was conducted using a stereomicroscope (Leica, S6E, Wetzlar, Germany) within a magnification range of 6.3× to 40×, equipped with a cold light source of 8 V/20 W. All particles suspected to have an organic origin, such as seed capsules, were extracted and stored separately. Subsequently, the presumed anthropogenic particles were documented under a digital microscope (Keyence, VHX-7000, Osaka, Japan) within a magnification range of 20× to 1000×, using a 4K CMOS camera. The length (i.e., the longest dimension), width (i.e., the shortest dimension), shape, and color of the particles were documented. For the categorization of the particles, various shape categories were established. This selection was based on a thorough examination of the shapes occurring in the samples of this study, taking into account the shapes that plastic particles can generally have. Furthermore, a careful evaluation of relevant literature sources was conducted [25–28]. In this study, six shape categories were distinguished: item (a), stick (b), string (c), fragment (d), pellet (e), and foil (f). Example images of these categories taken with a digital microscope are presented in Figure 3.

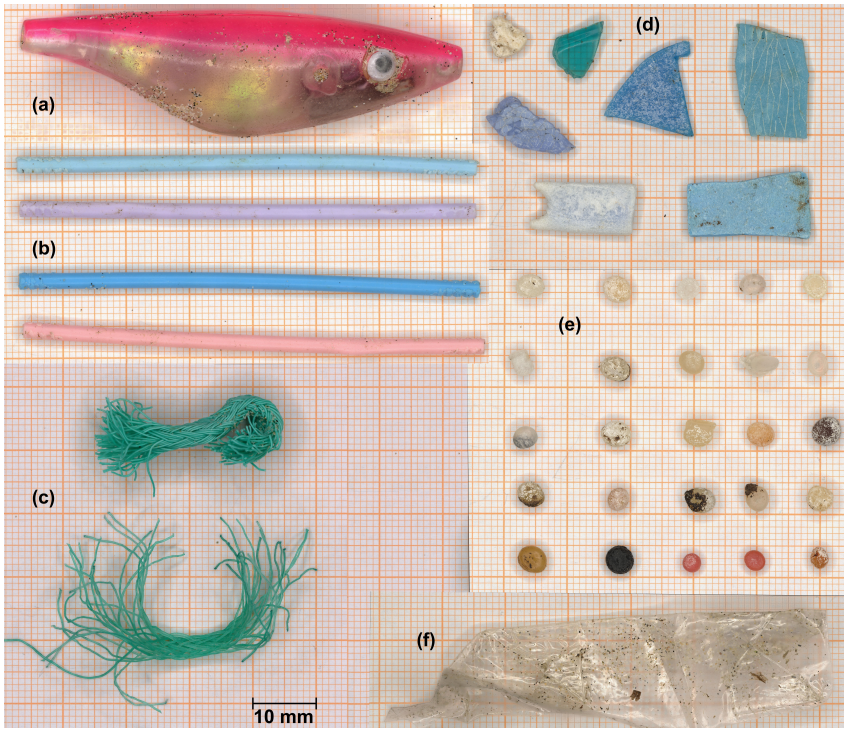

Figure 3. Digital microscopic images of plastic particles. The six distinguished shape categories are item (**a**), stick (**b**), string (**c**), fragment (**d**), pellet (**e**), and foil (**f**). The particles were placed on millimeter paper and a scale was inserted.

2.6. ATR-FTIR Spectroscopy

Each particle was analysed using an ATR-FTIR spectrometer (Perkin Elmer, Spectrum Two, Waltham, MA, USA) equipped with a lithium tantalate mid-infrared (MIR) detector and a diamond window. The ATR-FTIR spectra were recorded in the range of 400 cm^{-1} to 4000 cm^{-1} with a spectral resolution of 8 cm^{-1} using the Perkin Elmer Spectrum 10 STD software. Subsequently, the spectra were compared with various libraries to identify the chemical composition of the particles. Libraries from Perkin Elmer and ST Japan (Polymer ATR Starter Library L30002-2) were acquired, containing spectra of polymers and plastic-related components (e.g., additives, plasticizers, coatings). Commercial libraries contain references from newly manufactured materials. The particles themselves, especially their surfaces, undergo changes due to environmental influences, making it challenging to match them with the spectrum of brand-new polymers in the library. Therefore, in preliminary work, a dedicated library was created, encompassing plastic particles from various environmental matrices. In total, each particle was compared with 12.441 spectra. Only spectra with a match of at least 80 % were considered [44]. For lower matches, the spectrum was manually evaluated. All suspected organic particles could be confirmed as such. Suspected plastic particles that could not be identified but were definitively non-organic in origin were documented separately.

2.7. Differential Scanning Calorimetry (DSC)

Differential Scanning Calorimetry (DSC) is a thermal measurement technique that provides information on the amount of heat absorbed or released by a sample during isothermal operation, heating, or cooling. It measures not only endothermic and exothermic first-order transitions (such as melting and crystallization) but also second-order transitions (such as the glass transition temperature) and the enthalpy of a substance under various thermal conditions. This method allows for precise identification and differentiation between certain types of polymers [24]. Particles that could not be identified through ATR-FTIR spectroscopy were examined using DSC. For this purpose, a calorimeter (Netzsch, DSC 214 Polyma, Selb, Germany) with a ring sensor was employed at a heating rate of 10 $K\,min^{-1}$. The data were analysed using Netzsch software (Proteus 8.0).

2.8. Statistical Evaluation

The statistical analysis, figures, and charts were created using LaTeX, Excel [47], Inkscape 1.3.2 [48], and Python 3.8.10 [49] with the modules pandas [50,51], openpyxl [52], lat_lon_parser [53], matplotlib [54], and folium [42]. An imbalanced distribution of variables is a common phenomenon in data analysis. In this study, a sampling method was employed where the beaches were selectively investigated, leading to an under-representation of minorities. Therefore, in addition to box plots, kernel density estimation in the form of violin plots was used to model the distribution of a variable based on a random sample [55]. In comparison to box plots, violin plots may provide additional information about the frequency distribution of all data, akin to bar charts. Further information about violin plots can be found, for example, in [56–58].

3. Results

In this section, the distribution of plastic particles and their characteristics in beach sediments along the Côte d'Argent is presented. An overview is provided covering the entire coast from Plage Océane Port Médoc to Plage du Métro. In total, 14 beach sections with 70 sampling sites were investigated. This corresponds to a sample mass of beach sand of approximately 870 l or 1300 kg, assuming a mean density of 1.5 $g\,cm^{-3}$ [59] for the beach sediment. From the total sample mass, 1972 plastic particles were extracted. This averages to 1.5 particles kg^{-1} of beach sediment. The dominant shape categories were pellets ($N = 885$), and the predominant polymer type was polyethylene (PE) ($N = 1349$), constituting 45 % (pellets) and 68 % (PE) of all plastic particles, respectively.

3.1. Distribution

Figure 4 depicts a bar chart showing the number of extracted plastic particles for each individual beach, along with the median of the total quantity.

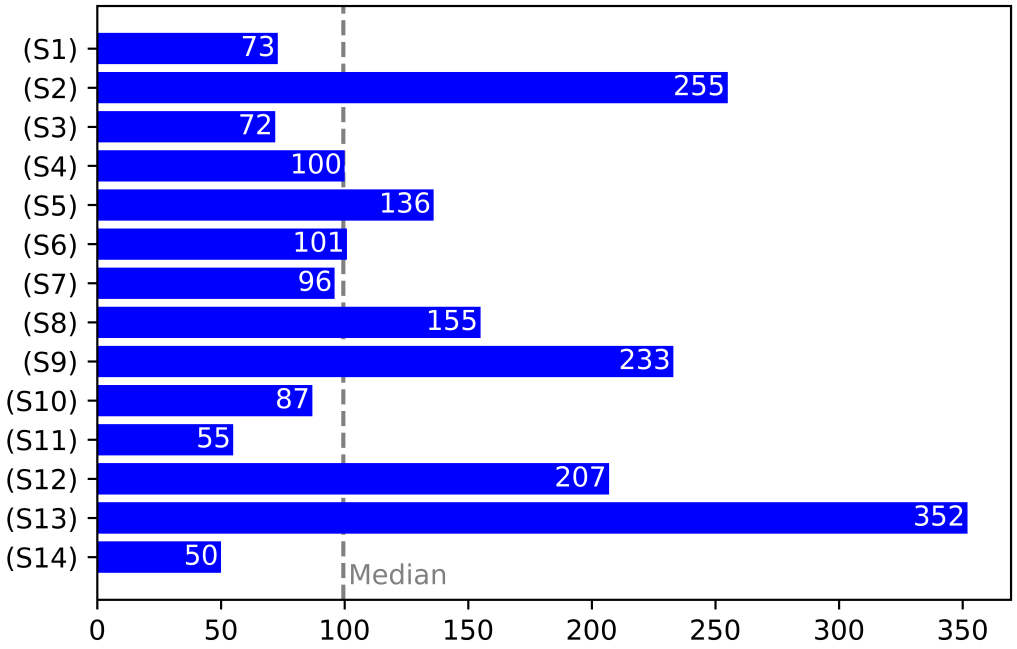

Figure 4. Bar chart illustrating the total number of particles found for each beach.

Except for one sampling site (Petri dish number 51) in transect S1, plastic particles were found at all other sampling sites. The highest number of plastic particles, with $N = 352$, was discovered at S13. The fewest plastic particles, totaling $N = 50$, were found at S14. The median number of plastic particles found on the beaches was 99.5. The total mass was 288 g. With an examined volume of roughly 0.8 m^3 (or 1300 kg) of beach sediment, this corresponds to a proportion of 0.2 ‰ or 1.5 particles kg^{-1}. One sample (Petri dish number 84) from S13 contained the highest weight of 25 g and also the most particles, totaling $N = 352$. The lightest sample from a single sampling site was from S2 (Petri dish number 124) with a mass of 1.3 g. In Figure 5, the statistical representation of all samples, showing the number of extracted plastic particles from each sample (Petri dish), is depicted in the form of box and violin plots. The violin plot provides an estimation of the core density on both sides of the distribution, thus illustrating the density distribution of the data. The box plots encompass the median, the 75th and 25th percentiles, with whiskers extending over 1.5 times the interquartile range. From Figure 5, it can be observed that the median is at 21 particles (orange line). However, the mean is at 27 particles per Petri dish (blue line), with the 75th and 25th percentiles at 12.5 and 37 particles (ends of the box), respectively. There are four outliers with particle counts of 80, 93, 110, and 126 (black circles) in a single sample. The violin plot (blue area) illustrates the frequency distribution of particles across the Petri dishes, with the frequency maximum observed at 17 particles. This could be interpreted as the estimated number of particles most commonly found across a large number of Petri dishes.

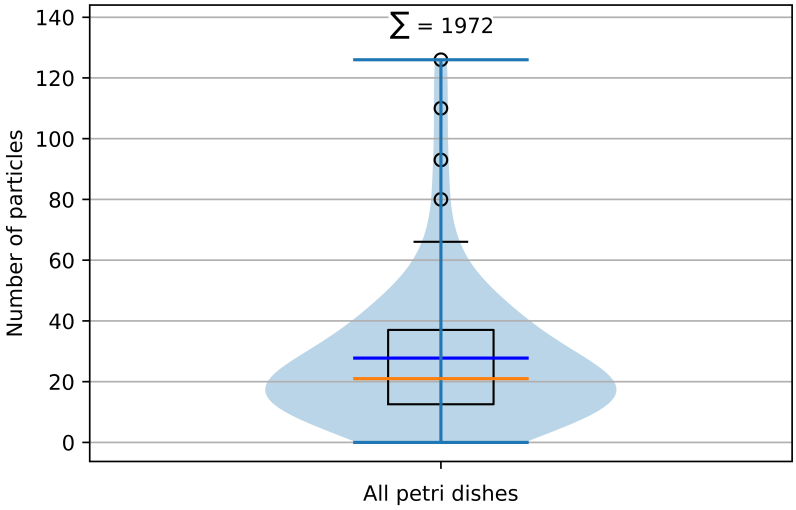

Figure 5. Statistical representation of the number of plastic particles extracted per Petri dish. The orange line depicts the median, while the blue line illustrates the mean. The box extends between the 75th and 25th percentiles. Outliers are indicated by black circles, and the violin plot is represented by the blue area.

3.2. Size

When categorising the data by size, it was observed that plastic particles with a count of $N = 943$ (47.8 %) were primarily present in samples ranging from 1 mm to 5 mm (microplastic particles). 863 particles (43.8 %) belonged to the mesoplastic size range of 5 mm to 25 mm. Macroplastics were least encountered, with 166 particles, belonging to the size range of 25 mm to 1000 mm. Figure 6 illustrates the statistical representation of all Petri dishes with the number of extracted plastic particles from each sample categorised by size (micro-, meso-, macroplastics) in the form of box and violin plots.

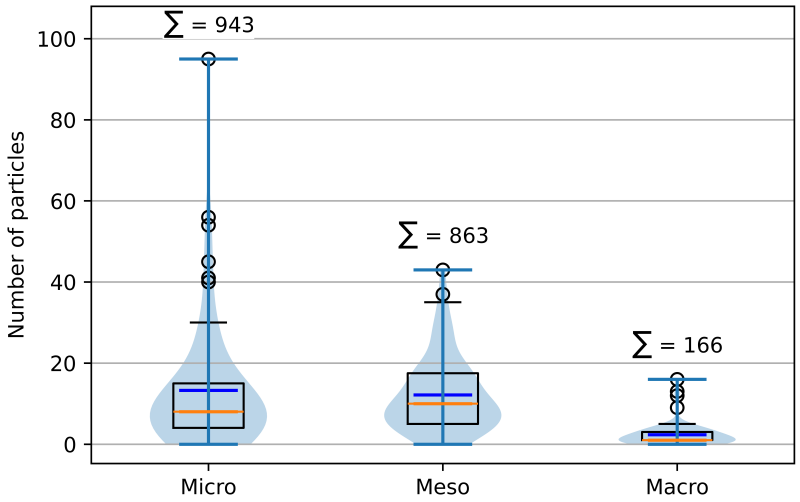

Figure 6. Statistical representation of the number of extracted plastic particles categorised by size (micro-, meso-, macroplastics) in the samples. The orange line depicts the median, while the blue line illustrates the mean. The box extends between the 75th and 25th percentiles. Outliers are indicated by black circles, and the violin plot is represented by the blue area.

Figure 7 illustrates the percentage distribution of the different size categories based on the sampled beaches. S14 had the lowest amount of detected microplastics and the highest number of mesoplastics. In comparison to other beaches, the directly adjacent beaches, S6 and S9, had the lowest amount of macroplastics.

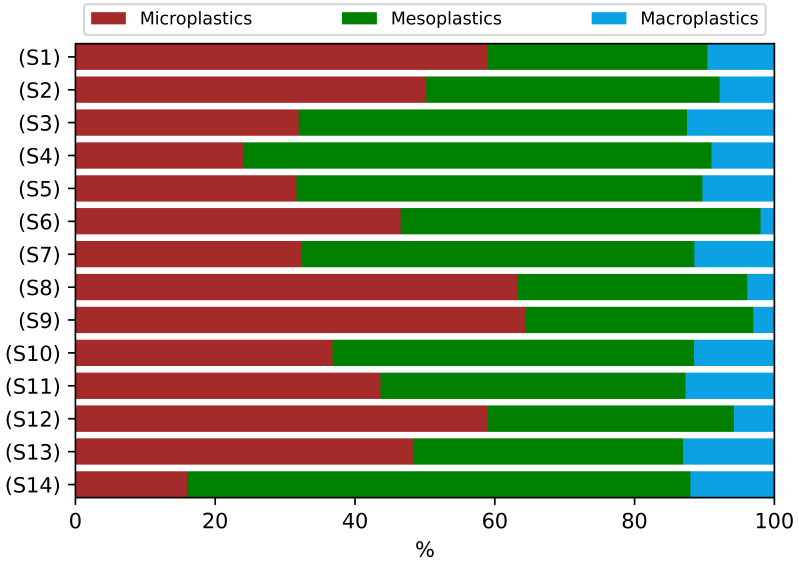

Figure 7. Percentage distribution of microplastics, mesoplastics, and macroplastics at different beaches.

3.3. Shape Categories

In Figure 8, various shape categories are assigned to different beaches in different colors, along with their respective percentage distributions. Pellets and fragments were the most prevalent in the samples, with 885 and 861 plastic particles, respectively. They were followed by items ($N = 110$), strings ($N = 51$), sticks ($N = 50$), and foils ($N = 15$). Thus, pellets dominated at all sampling sites, constituting 44.9 % of the particles. Foils were found at the fewest beaches and were concentrated at the S5 sampling site. No sticks were found at beaches S5, S6, and S14.

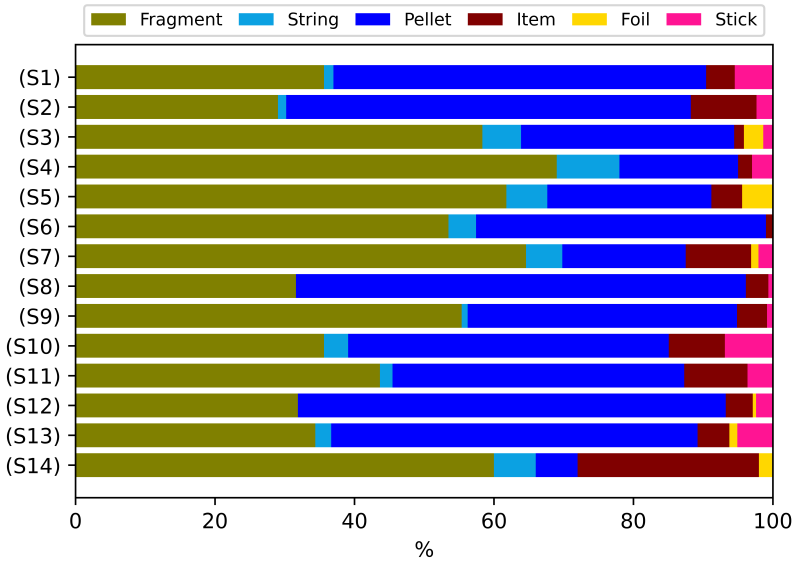

Figure 8. Percentage distribution of shape categories at sampled beaches. Pellets (44.9 %) and fragments were the most common, followed by items, sticks, strings, and foils.

In Figures 9 and 10, the number of all plastic particles extracted from the samples is depicted based on shape categories (fragment, string, pellet, item, foil, stick) as box and violin plots. The violin plot of the fragments indicates that frequencies were mainly in the range of 0 to 20 particles, with very few Petri dishes containing a higher number of particles. The violin plot of the pellets shows a wide distribution of lower frequencies, with the most common being 0 to 12 pellets found. However, compared to the fragments, it clearly shows

more frequent particle occurrences above 20 particles, with outliers exhibiting significantly higher particle quantities. The median (orange line) for fragments was $N = 10$, and for pellets, it was $N = 8$, with the mean (blue line) for both being 12 particles. The frequency distribution is also very similar, with nine particles for fragments and seven particles for pellets. In Figure 10, for the string, foil, and stick shapes, a different scaling of the ordinate was chosen as significantly fewer particles were found compared to fragments and pellets. Strings, foils, and sticks were very rarely or not found at all, with the frequency maximum (and also mean or median) being in the range of 0 to 1 particles. In comparison, items were found much more frequently, with an average of one particle per Petri dish, and larger values also occurring, showing a flat decrease in frequency up to four particles per Petri dish.

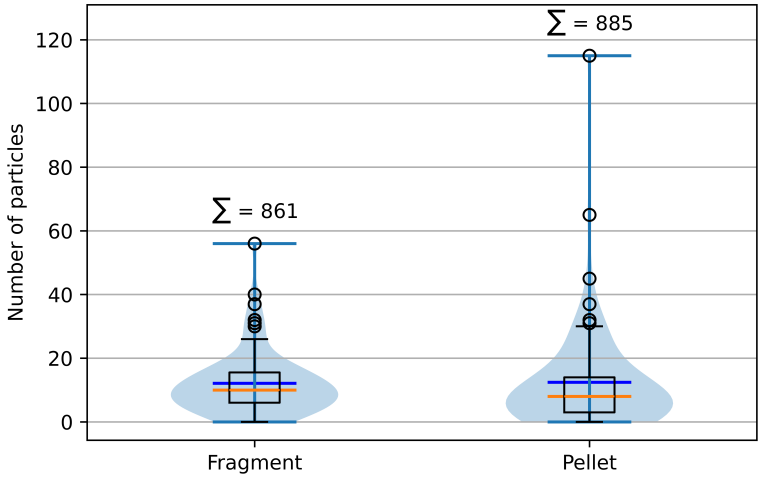

Figure 9. Box and violin plots of all extracted particles in the shape categories of fragment and pellet. The orange line depicts the median, while the blue line illustrates the mean. The box extends between the 75th and 25th percentiles. Outliers are indicated by black circles, and the violin plot is represented by the blue area.

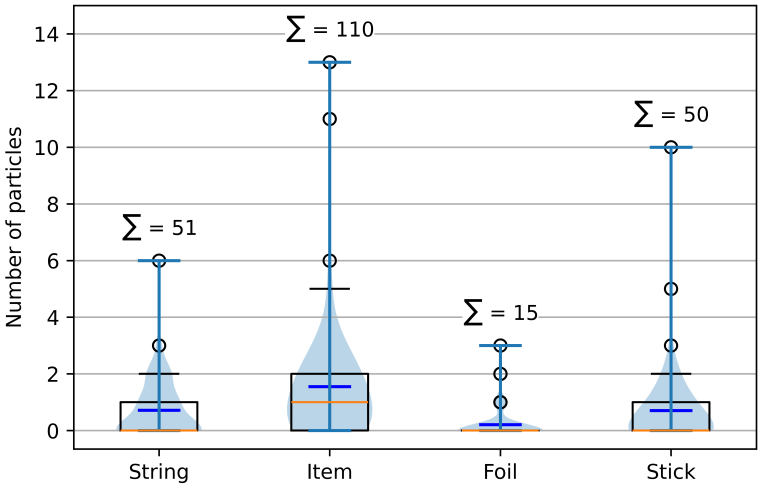

Figure 10. Box and violin plots of all extracted particles in the shape categories of string, item, foil, and stick. The orange line depicts the median, while the blue line illustrates the mean. The box extends between the 75th and 25th percentiles. Outliers are indicated by black circles, and the violin plot is represented by the blue area.

3.4. Color

Figure 11 illustrates the percentage distribution of different color categories at the sampled beaches. The majority of plastic particles, totaling 1226, consisted of white particles,

comprising 62.1 % of the total. The predominant portion of white particles was white-translucent, with $N = 856$ (43.4 %), of which 71.5 % ($N = 612$) were pellets alone. Blue was also quite prevalent, with 174 plastic particles, but only 6.3 % ($N = 11$) of these were pellets; primarily, fragments with 131 particles were found. At beach S10, no black particles were found, distinguishing it from the others. Transparent plastic particles, on the other hand, were only detected at nine out of the 14 beaches.

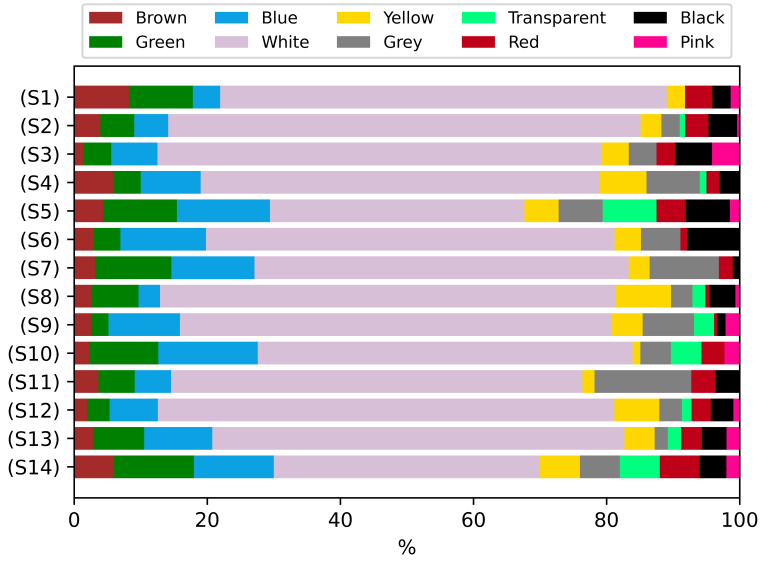

Figure 11. The amount and distribution of different color categories.

3.5. Identification

Figure 12 provides an overview of the percentage distribution of different polymer categories at the examined beaches. Regardless of the sampling location, PE was the most frequently found polymer, constituting 68.4 % ($N = 1349$) of the total. It was followed by polypropylene (PP) at 25.8 % ($N = 508$) and polystyrene (PS) at 3.1 % ($N = 61$) plastic particles. At beaches S11 and S8, only PP and PE plastic particles were detected, in contrast to the other beaches. Beach S14 had the lowest number of PE particles, with $N = 12$, but it had the highest number of PS particles, also with $N = 12$. Out of a total of 1972 plastic particles, $N = 26$ could not be definitively identified; these particles were mostly visually identified as weathered foam. Additionally, 13 particles were identified as organic during pre-sorting, mostly seed capsules or fragments of shells. These were further examined using ATR-FTIR spectroscopy and confirmed as non-anthropogenic.

3.6. DSC Measurements

Additionally, nine plastic particles that could not be identified using ATR-FTIR spectroscopy were examined with DSC. Only four of them could be identified using DSC but with an uncertain correlation factor of less than 80 %. These particles were heavily weathered and mixed with sand, soil, and organic material, making a clear assignment challenging. Therefore, these particles continued to be classified as "not identified". The differentiation between Low-Density Polyethylene (LDPE) and High-Density Polyethylene (HDPE) using ATR-FTIR spectroscopy proved to be unreliable. To gain an overview of the distribution, an additional 10 PE pellets were randomly selected (from various Petri dishes) and analysed using DSC. Seven pellets were identified as LDPE, and three pellets as HDPE. In relation to the total number of PE pellets found (711 particles or 36.1 %), this would correspond to 497 LDPE pellets. However, a sample size of 1.5 % lacks statistical significance and serves only as a rough estimate.

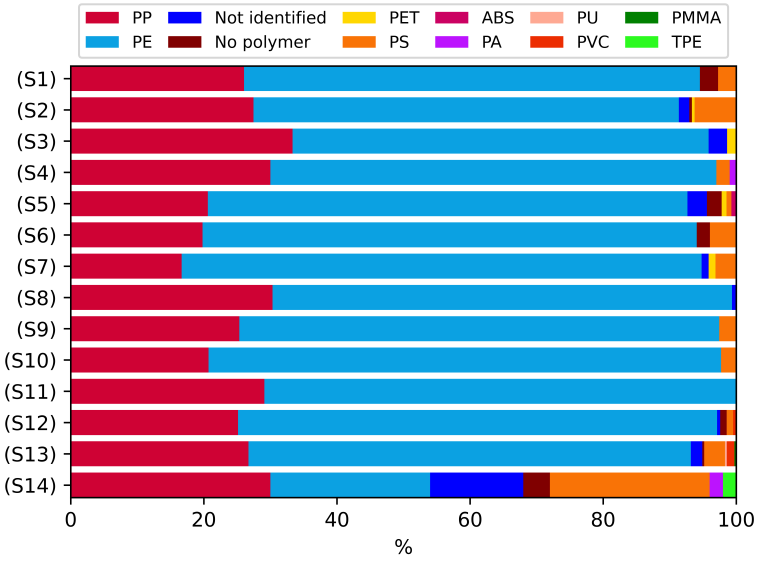

Figure 12. Bar chart depicting various polymer categories, sampled beaches, and their respective percentage distribution.

4. Discussion

4.1. Distribution

A short overview of plastic pollution in beach sand or sediments, mainly in Europe, is given in Table 2 for comparison purposes. As can be seen, many beach sand sediments and sediment samples have significantly higher values compared to this study: The range of occurrence of plastic particles is very wide, ranging from 0 particles kg^{-1} to 2457 particles kg^{-1}. Sampling methods are also extremely diverse, as there are currently no standardized methods, which complicates comparability. Besides possible geographical sampling site divergences (e.g., different degrees of pollution), for example, in comparison to the distribution at a similar beach section investigated in this study, Bassin d'Arcachon in France was examined [33], where 6 particles kg^{-1} were found. The concentration measured here of 1.5 particles kg^{-1} for Côte d'Argent is of the same order of magnitude. One possible reason for the slightly higher concentration found in the study by Lefebvre et al. [33] is that the present study includes microplastic particles of very small size (<1 mm). In comparison, this size was not included in the aforementioned study, and, therefore, a significant amount of particles may not have been detected. This needs to be investigated further for clarification.

On average, the distribution of plastic particles was similar at all beaches. The only exception in the distribution was beach S13, which had a significantly higher number of plastic particles, with $N = 352$, in comparison to the other beaches. The reason for the significantly higher quantity at this beach section could not be determined. The Bassin d'Arcachon is connected to the Atlantic Ocean. At the mouth, two main channels, the North Channel (outflow) and the South Channel (inflow), connect the bay to the ocean, facilitating water circulation. Approximately two-thirds of the water volume is renewed during each tidal cycle [60]. Sampling site S9 is located at the South Channel, whereas sampling sites S7 and S8 are located at the North Channel (see Figure 2). The distribution of particles indicates that there are significantly more particles (S9 $N = 233$) at the South Channel, the inflow, compared to the North Channel, the outflow (S7 $N = 96$ and S8 $N = 155$). This may suggest that currents are carrying plastic waste into the bay, where it accumulates [37].

Table 2. Overview of plastic pollution in beach sand or sediments in various coastal regions worldwide.

Region		Abundance	Unit	Reference
Eastern Argentina		1693	particles kg^{-1}	[19]
Southern Morocco	(2018)	915	particles kg^{-1}	[20]
	(2019)	1448	particles kg^{-1}	
Eastern Morocco		40 to 230	particles kg^{-1}	[61]
Western Algerian		55	particles m^{-2}	[21]
Caribbean beaches		557 to 2457	particles kg^{-1}	[22]
East Chinese		664	particles kg^{-1}	[23]
Northern Slovenia		23	particles kg^{-1}	[25]
Northeast Thailand		6 to 81	particles kg^{-1}	[26]
West France		67	particles kg^{-1}	[38]
West France		13.5	particles kg^{-1}	[37]
West France		6	particles kg^{-1}	[33]
South France		80	particles l^{-1}	[34]
Southwest Turkey		63 to 379	particles kg^{-1}	[62]
West Scotland		161 to 432	particles kg^{-1}	[63]
North Germany		1.8 to 30.2	particles kg^{-1}	[64]
Northwest Germany		2 to 4	particles kg^{-1}	[65]
South Australia		0.5 to 2	particles kg^{-1}	[66]
North Italy		6 to 26	particles kg^{-1}	[67]
North Greece		0 to 32	particles m^{-3}	[68]
Southeast Bangladesh		8	particles kg^{-1}	[44]

4.2. Size

The Atlantic Ocean has been investigated much more frequently than the French Atlantic coast. Typically, water samples are collected and analysed for plastic pollution in these studies, revealing a generally higher proportion of microplastics (80 %) and significantly fewer meso- and macroplastics [2]. In the present sampling, however, micro- and mesoplastics were approximately equally represented, accounting for 48 % and 45 % of the total, respectively. It is reasonable to assume that the number or proportion of identified microplastic particles in this study represents a lower estimate. This is due to the lower detection limit of 1 mm, which excluded all particles smaller than 1 mm from the sampling. Macroplastics were much less prominent in this sampling compared to the other two categories. The number or proportion of macroplastics should also be considered a lower estimate, as larger macroplastic pieces are regularly collected by municipal beach cleaning or cleanup initiatives.

4.3. Shape Categories

With a share of approximately 45 %, pellets comprised the majority of the particles. In Ref. [37], investigations at the same beach sections (S6 and S10) in 2021 revealed a pellet proportion ranging from 34 % to 50 %, which is comparable to the findings of this study (45 %). Analysis of the surfaces using digital microscopy during documentation revealed various aging states of the pellets. The most common pellets were white, had a smooth surface, and showed only slight signs of aging. This applied to 80 % of the pellets. In Ref. [46], 50 % of the discovered pellets were also identified as new, found in beach sediments collected consistently throughout the year at fixed locations [46]. This could indicate a short residence time in the marine environment [36,69]. In visually identified aged pellets, surface features such as cracks, material loss, erosion, adhesion, granulation, and color changes were observed. Among the remaining plastic particles, especially in the category "items", mainly marine debris was found. In contrast, a European Union study [16] in 2016 reported 50 % single-use plastic waste on European beaches. One possible influencing factor is tourism, which is less active in this area during the winter months. In combination with municipal beach cleanings, this could potentially lead to less packaging waste on the beaches. Another influencing factor is the elapsed time and the nature of the

last beach cleaning, which could result in overestimation or underestimation of the number or respective proportions [9]. However, it could not be determined how often the sampled beaches are cleaned during the winter months and when the last cleaning took place. A total of 50 sticks were found in the samples. Among the clearly identifiable sticks, 33 (66 % of the sticks) were cotton bud sticks, and one was a lollipop stick; however, 16 sticks (32 % of the sticks) could not be assigned. Due to the varying degrees of aging, the origin (new or waste) could not be definitively determined. In Ref. [70], cotton bud sticks were the most frequently found particles in the Golfe de Gascogne, accounting for 13.7 % along European coasts [16,70]. In contrast, foam sponges, plastic lids, and tangled nets/cords/ropes and strings were found much less frequently. Foils were comparatively rare, likely because they fragment into smaller particles more quickly and, therefore, do not fall within the detected size range [71].

4.4. Color

The characterization of the color of plastic particles is often a component of studies on plastic waste. In Ref. [72], a study conducted in the Golfe de Gascogne suggests that white and white-transparent plastic particles predominantly occur near the coast. The authors also found that as the distance from the coast increases toward the open sea and the size of the plastic particles decreases, the number of white particles decreases. The predominant color of all plastic particles in this study was also white, with the majority being white-translucent. This aligns with the results of other studies in the Golfe de Gascogne [37,72]. Overall, white, blue, and green were most the frequently found colors, which is common in marine waste. In another study conducted in Arcachon Bay [33], 45 % of particles found in beach sediment were black. However, it is essential to note that the study in Arcachon Bay focused on microplastic particles ranging from 17 µm to 5000 µm, whereas this study only partially considered such a size range, with a detection size ranging from 1 mm to 1000 mm. Another study investigating the Atlantic [73] also found predominantly black plastic particles, but it specifically examined the micro-range (<1 mm). Since this size range was not explored in the current study, it can be assumed that the actual number of black particles in beach sediment was underestimated. Therefore, it appears that black is the prevalent color in smaller particles, and its frequency decreases for particles larger than 1 mm. Furthermore, it is noticeable that the majority of unidentified particles here were black. One possible reason for this may lie in the fact that identifying the plastic type in black plastic particles is generally more challenging using ATR-FTIR spectroscopy [32,74]. It can be assumed that polymer fragmentation mechanisms generally differ between bright and dark colors. This is because the aging of bright plastics is predominantly attributed to UV radiation, whereas dark plastics undergo aging due to a combination of UV radiation and thermooxidation processes, as they absorb more heat from the sun [29].

4.5. Identification

The most commonly occurring polymer groups in the environment—PE, PP, and PS—represent the most widely used commodity plastics, primarily utilised for packaging. In the EU, plastics account for 80 % to 85 % of anthropogenic marine litter, with 50 % of it being single-use products [18,30,72]. Polyamide (PA), polymethyl methacrylate (PMMA), polyurethane (PU), and polyvinyl chloride (PVC) are also common, but numerically less significant compared to PE and PP [73]. In this study, all of these polymer groups were found, with PE and PP being by far the most prevalent. In a study on the Côte d'Argent [75], mussels were examined for particle sizes ranging from 50 µm to 100 µm. The main polymer types detected were PE and PP; however, a significant amount of acrylonitrile butadiene styrene (ABS) was also found, which was barely present in this study with one particle. On average, the polymer groups were equally distributed across all beaches, except for beach S14, which deviated from the overall distribution. Here, larger quantities of PS were found, along with the majority of unidentified polymers. The PS particles consisted of white expanded PS, which could originate from a single source. Furthermore, this beach was the

only one where thermoplastic elastomer (TPE) was found. All unidentified particles were made of neon-green foam, visually and spectroscopically identified as the same material. This raises the question of whether the widespread distribution of these polymer types (on beach S14) is artificial, as these are large objects that may have fragmented on the beach. Considering that these materials are also used for kite and surf equipment and these sports are particularly popular on this beach, the high contamination may originate from these activities [76].

4.6. DSC Analysis

It was found that DSC can serve as a supplementary analytical method when ATR-FTIR spectroscopy results are uncertain or when analysis is not possible [77]. DSC was able to clearly distinguish between LDPE and HDPE. For the particles that could not be identified with ATR-FTIR ($N = 9$), DSC measurements also could not yield a clear identification. Most of these particles consisted of neon-green foam. As DSC did not show melting processes for these particles, it can be assumed that they consist of an elastomeric polymer, which is generally difficult to identify with DSC. Furthermore, DSC is a destructive analytical method, where measurement runs typically take one to two hours, in contrast to only a few minutes for an ATR-FTIR spectroscopy measurement. Therefore, it should not be the primary choice.

5. Conclusions

In 2016, 84 % of waste found along European coasts consisted of plastic [16]. Understanding the composition and distribution patterns of waste in different environmental matrices is crucial for identifying its origin and developing effective measures [16]. This study examined 250 km of coastline at 70 sampling sites. With a total analysed matrix weight of approximately 1300 kg of beach sediment, 1972 plastic particles were found and investigated, providing a comprehensive overview of plastic pollution on the Côte d'Argent. The exclusion of particles smaller than 1 mm and larger than 1000 mm from the study suggests that the calculated 1.5 particles kg^{-1} of beach sediment might be an underestimation. Pellets ($N = 885$) dominated as the form category, followed by fragments ($N = 861$). The most prevalent polymer type was polyethylene ($N = 1349$), followed by polypropylene ($N = 508$). White/white-translucent emerged as the most common color, with 1226 particles. The particles mainly identified as pellets in this study indicate that pellet loss plays a significant role in beach pollution, even more than waste from tourism, at least outside the tourist season. Pellets have never been produced into a product and, therefore, provide no societal value. These findings underscore the need for ways to prevent plastic pellet loss into the environment.

Author Contributions: Conceptualization, D.B. and J.S.; methodology, D.B. and J.S.; software, D.B.; formal analysis, D.B.; investigation, D.B. and J.S.; writing—original draft preparation, D.B. and J.S.; writing—review and editing, J.S.; visualization, D.B.; supervision, J.S.; project administration, J.S. All authors have read and agreed to the published version of the manuscript.

Funding: This research received no external funding.

Institutional Review Board Statement: Not applicable.

Informed Consent Statement: Not applicable.

Data Availability Statement: The raw data supporting the conclusions of this article will be made available by the authors upon request.

Acknowledgments: We are very grateful for the informative discussion and advice provided by Charlotte Lefebvre, who has significant expertise in investigating plastic pollution in the area of Arcachon Bay and the surrounding shores. We also greatly appreciate the discussion and valuable insights provided by Gerd Knupp regarding this publication. We extend our sincere gratitude to Marcel Bornstein for his invaluable assistance with Python programming.

Conflicts of Interest: The authors declare no conflicts of interest.

Abbreviations

The following abbreviations are used in this manuscript:

EU	European Union
ATR-FTIR spectroscopy	Attenuated Total Reflectance-Fourier Transform Infrared Spectroscopy
GPS	Global Positioning System
MIR	Mid-infrared
DSC	Differential Scanning Calorimetry
PE	Polyethylene
PP	Polypropylene
PS	Polystyrene
PET	Polyethylene terephthalate
LDPE	Low-Density Polyethylene
HDPE	High-Density Polyethylene
PA	Polyamide
PMMA	Polymethyl methacrylate
PU	Polyurethane
PVC	Polyvinyl chloride
ABS	Acrylonitrile Butadiene Styrene
TPE	Thermoplastic elastomer

References

1. Lechthaler, S.E. Microplastics in the Environment: Development of a Sample Preparation Method with Further Application and Evaluation in Fluvial and Marine Compartments. Ph.D. Thesis, Rheinisch-Westfälische Technische Hochschule Aachen, Aachen, Germany, 2021. [CrossRef]
2. Syberg, K.; Knudsen, C.M.; Tairova, Z.; Khan, F.R.; Shashoua, Y.; Geertz, T.; Pedersen, H.B.; Sick, C.; Mortensen, J.; Strand, J.; et al. Sorption of PCBs to environmental plastic pollution in the North Atlantic Ocean: Importance of size and polymer type. *Case Stud. Chem. Environ. Eng.* **2020**, *2*, 100062. [CrossRef]
3. McGlade, J.; Fahim, I.; Green, D.; Landrigan, P.; Andrady, A.; Costa, M.; Geyer, R.; Gomes, R.; Hwai, A.; Jambeck, J.; et al. *From Pollution to Solution: A Global Assessment of Marine Litter and Plastic Pollution*; Technical Report; United Nations Environment Programme: Nairobi, Kenya, 2021. [CrossRef]
4. Allen, D.; Allen, S.; Maselli, V.; LeBlanc, A.; Kelleher, L.; Krause, S.; Walker, T.; Ryan, A. Hurricane transport of ocean-sourced microplastic in the North Atlantic. *Commun. Earth Environ.* **2023**, *4*, 442. [CrossRef]
5. Barrio Froján, C.; Bergmann, M.; Woodall, L.; C. Mestre, N.; Baker, M.; Gertz, B.; Escobar-Briones, E.; Ekpe, S.; Pham, C.; Martins, I.; et al. Plastic Pollution in the Deep Ocean. In *DOSI Policybrief Deep-Ocean Stewardship Initiative*; DOSI: Southampton, UK, 2023.
6. Ritchie, H. How Much Plastic Waste Ends Up in the Ocean? Our World in Data. 2023. Available online: https://ourworldindata.org/how-much-plastic-waste-ends-up-in-the-ocean (accessed on 19 January 2024).
7. Papadimitriu, M.; Allinson, G. Microplastics in the Mediterranean marine environment: A combined bibliometric and systematic analysis to identify current trends and challenges. *Microplast. Nanoplast.* **2022**, *2*, 25. [CrossRef]
8. Allen, S.; Materić, D.; Allen, D.; MacDonald, A.; Holzinger, R.; Roux, G.L.; Phoenix, V.R. An early comparison of nano to microplastic mass in a remote catchment's atmospheric deposition. *J. Hazard. Mater. Adv.* **2022**, *7*, 100104. [CrossRef]
9. Rochman, C.; Andrady, A.; Dudas, S.; Fabres, J.; Galgani, F.; Hardesty, D.; Hidalgo-Ruz, V.; Hong, S.; Kershaw, P.; Lebreton, L.; et al. *Sources, Fate and Effects Of Microplastics in the Marine Environment: Part 2 of A Global Assessment*; Technical Report; International Maritime Organization: London, UK, 2016.
10. Beck, A.; Borchert, E.; Delaigue, L.; Deng, F.; Gueroun, S.; Hamm, T.; Jacob, O.; Kaandorp, M.; Hashan, K.; Kossel, E.; et al. *NAPTRAM—Plastiktransportmechanismen, Senken und Interaktionen mit Biota im Nordatlantik/NAPTRAM—North Atlantic Plastic Transport Mechanisms, Sinks, and Interactions with Biota, Cruise No. SO279, Emden (Germany)—Emden (Germany), 04.12.2020–05.01.2021*; Technical Report; GEOMAR Helmholtz Centre for Ocean Research Kiel: Bonn, Germany, 2021. [CrossRef]
11. Okoffo, E.D.; O'Brien, S.; Ribeiro, F.; Burrows, S.D.; Toapanta, T.; Rauert, C.; O'Brien, J.W.; Tscharke, B.J.; Wang, X.; Thomas, K.V. Plastic particles in soil: State of the knowledge on sources, occurrence and distribution, analytical methods and ecological impacts. *Environ. Sci. Process. Impacts* **2021**, *23*, 240–274. [CrossRef] [PubMed]
12. Hassan, Y.; Badrey, A.; Osman, A.; Mahdy, A. Occurrence and distribution of meso- and macroplastics in the water, sediment, and fauna of the Nile River, Egypt. *Environ. Monit. Assess.* **2023**, *195*, 1130. [CrossRef]

13. Alava, J.J.; Moreno-Baez, M.; McMullen, K.; Tekman, B.; Barrows, A.; Bergmann, M.; Price, D.; Swartz, W.; Ota, Y. *Ecological Impacts of Marine Plastic Pollution, Microplastics Foodweb Bioaccumulation Modelling and Global Ocean Footprint: Insights into the Problems, the Management Implications and Coastal Communities Inequities. The Nippon Foundation-Ocean Litter Project (2019–2023)*; Technical Report; University of British Columbia: Vancouver, BC, Canada, 2023. [CrossRef]
14. Walkinshaw, C.; Lindeque, P.K.; Thompson, R.; Tolhurst, T.; Cole, M. Microplastics and seafood: lower trophic organisms at highest risk of contamination. *Ecotoxicol. Environ. Saf.* **2020**, *190*, 110066. [CrossRef] [PubMed]
15. Bertling, J.; Bertling, R.; Hamann, L. *Kunststoffe in der Umwelt: Mikro- und Makroplastik. Ursachen, Mengen, Umweltschicksale, Wirkungen, Lösungsansätze, Empfehlungen. Kurzfassung der Konsortialstudie*; Technical Report; Fraunhofer-Institut für Umwelt-, Sicherheits- und Energietechnik (UMSICHT): Oberhausen, Germany, 2018.
16. Addamo, A.; Laroche, P.; Hanke, G. *Top Marine Beach Litter Items in Europe a Review and Synthesis Based on Beach Litter Data*; Technical Report; Office of the European Union: Luxembourg, 2018. [CrossRef]
17. European Parliament; Council of the European Union. *Directive 2008/56/EC of the European Parliament and of the Council, Establishing a Framework for Community Action in the Field of Marine Environmental Policy (Marine Strategy Framework Directive)*; European Parliament: Strasbourg, France, 2008.
18. Pabortsava, K.; Lampitt, R.S. High concentrations of plastic hidden beneath the surface of the Atlantic Ocean. *Nat. Commun.* **2020**, *11*, 4073. [CrossRef] [PubMed]
19. Arias, A.H.; Alvarez, G.; Pozo, K.; Pribylova, P.; Klanova, J.; Rodríguez Pirani, L.S.; Picone, A.L.; Alvarez, M.; Tombesi, N. Beached microplastics at the Bahia Blanca Estuary (Argentina): Plastic pellets as potential vectors of environmental pollution by POPs. *Mar. Pollut. Bull.* **2023**, *187*, 114520. [CrossRef] [PubMed]
20. Ben-Haddad, M.; Abelouah, M.R.; Hajji, S.; Rangel-Buitrago, N.; Hamadi, F.; Alla, A.A. Microplastics pollution in sediments of Moroccan urban beaches: The Taghazout coast as a case study. *Mar. Pollut. Bull.* **2022**, *180*, 113765. [CrossRef] [PubMed]
21. Bentaallah, M.E.A.; Baghdadi, D.; Gündoğdu, S.; Megharbi, A.; Taibi, N.E.; Büyükdeveci, F. Assessment of microplastic abundance and impact on recreational beaches along the western Algerian coastline. *Mar. Pollut. Bull.* **2024**, *199*, 116007. [CrossRef] [PubMed]
22. Rangel-Buitrago, N.; Arroyo-Olarte, H.; Trilleras, J.; Arana, V.A.; Mantilla-Barbosa, E.; Gracia C., A.; Mendoza, A.V.; Neal, W.J.; Williams, A.T.; Micallef, A. Microplastics pollution on Colombian Central Caribbean beaches. *Mar. Pollut. Bull.* **2021**, *170*, 112685. [CrossRef]
23. Pervez, R.; Lai, Y.; Song, Y.; Li, X.; Lai, Z. Impact of microplastic pollution on coastal ecosystems using comprehensive beach quality indices. *Mar. Pollut. Bull.* **2023**, *194*, 115304. [CrossRef] [PubMed]
24. Sorolla-Rosario, D.; Llorca-Porcel, J.; Pérez-Martínez, M.; Lozano-Castelló, D.; Bueno-López, A. Study of microplastics with semicrystalline and amorphous structure identification by TGA and DSC. *J. Environ. Chem. Eng.* **2022**, *10*, 106886. [CrossRef]
25. Matjašič, T.; Mori, N.; Hostnik, I.; Bajt, O.; Kovač Viršek, M. Microplastic pollution in small rivers along rural–urban gradients: Variations across catchments and between water column and sediments. *Sci. Total. Environ.* **2023**, *858*, 160043. [CrossRef] [PubMed]
26. Kasamesiri, P.; Panchan, R.; Thaimuangphol, W. Spatial–Temporal Distribution and Ecological Risk Assessment of Microplastic Pollution of Inland Fishing Ground in the Ubolratana Reservoir, Thailand. *Water* **2023**, *15*, 330. [CrossRef]
27. Al., I.A.E. Microplastic Pollution in Turkish Aquatic Ecosystems: Sources, Characteristics, Implications, and Mitigation Strategies. *Turk. J. Fish. Aquat. Sci.* **2023**, *23*, TRJFAS24773.
28. Li, Y.; Lu, Q.; Yang, J.; Xing, Y.; Ling, W.; Liu, K.; Yang, Q.; Ma, H.; Pei, Z.; Wu, T.; et al. The fate of microplastic pollution in the Changjiang River estuary: A review. *J. Clean. Prod.* **2023**, *425*, 138970. [CrossRef]
29. Huang, Y.; Xu, E.G. Black microplastic in plastic pollution: Undetected and underestimated? *Water Emerg. Contam. Nanoplast.* **2022**, *1*, 14. [CrossRef]
30. Kadac-Czapska, K.; Knez, E.; Gierszewska, M.; Olewnik-Kruszkowska, E.; Grembecka, M. Microplastics Derived from Food Packaging Waste-Their Origin and Health Risks. *Materials* **2023**, *16*, 674. [CrossRef] [PubMed]
31. Mariano, S.; Tacconi, S.; Fidaleo, M.; Rossi, M.; Dini, L. Micro and Nanoplastics Identification: Classic Methods and Innovative Detection Techniques. *Front. Toxicol.* **2021**, *3*, 636640. [CrossRef]
32. Debbarma, N.; Gurjar, U.R.; Ramteke, K.K.; Shenoy, L.; Nayak, B.B.; Bhushan, S.; Geethalakshmi, V.; Xavier, M. Abundance and characteristics of microplastics in gastrointestinal tracts and gills of croaker fish (Johnius dussumieri) from off Mumbai coastal waters of India. *Mar. Pollut. Bull.* **2022**, *176*, 113473. [CrossRef] [PubMed]
33. Lefebvre, C.; Le Bihanic, F.; Jalón-Rojas, I.; Dusacre, E.; Chassaigne-Viscaïno, L.; Bichon, J.; Clérandeau, C.; Morin, B.; Lecomte, S.; Cachot, J. Spatial distribution of anthropogenic particles and microplastics in a meso-tidal lagoon (Arcachon Bay, France): A multi-compartment approach. *Sci. Total. Environ.* **2023**, *898*, 165460. [CrossRef] [PubMed]
34. Cutroneo, L.; Capello, M.; Domi, A.; Consani, S.; Lamare, P.; Coyle, P.; Bertin, V.; Dornic, D.; Reboa, A.; Geneselli, I.; et al. Microplastics in the abyss: A first investigation into sediments at 2443-m depth (Toulon, France). *Environ. Sci. Pollut. Res.* **2022**, *29*, 9375–9385. [CrossRef] [PubMed]
35. Mancuso, M.; Genovese, G.; Porcino, N.; Natale, S.; Crisafulli, A.; Spagnuolo, D.; Catalfamo, M.; Morabito, M.; Bottari, T. Psammophytes as traps for beach litter in the Strait of Messina (Mediterranean Sea). *Reg. Stud. Mar. Sci.* **2023**, *65*, 103057. [CrossRef]

36. Giugliano, R.; Cocciaro, B.; Poggialini, F.; Legnaioli, S.; Palleschi, V.; Locritani, M.; Merlino, S. Rapid Identification of Beached Marine Plastics Pellets Using Laser-Induced Breakdown Spectroscopy: A Promising Tool for the Quantification of Coastal Pollution. *Sensors* **2022**, *22*, 6910. [CrossRef]
37. Lefebvre, C.; Rojas, I.J.; Lasserre, J.; Villette, S.; Lecomte, S.; Cachot, J.; Morin, B. Stranded in the high tide line: Spatial and temporal variability of beached microplastics in a semi-enclosed embayment (Arcachon, France). *Sci. Total. Environ.* **2021**, *797*, 149144. [CrossRef]
38. Phuong, N.N.; Poirier, L.; Lagarde, F.; Kamari, A.; Zalouk-Vergnoux, A. Microplastic abundance and characteristics in French Atlantic coastal sediments using a new extraction method. *Environ. Pollut.* **2018**, *243*, 228–237. [CrossRef] [PubMed]
39. Nowaczyk, A.; Vincent, D.; Curd, A.; Antajan, E.; Masse, C. Invasion along the French Atlantic coast by the non-native, carnivorous planktonic comb jelly Mnemiopsis leidyi: Can an impact on shellfish farming be expected? *Bioinvasions Rec.* **2023**, *12*, 371–384. [CrossRef]
40. Westfälische, N. Frankreichs Justiz ermittelt Wegen Plastikgranulats an der Atlantikküste. 2023. Available online: https://www.nw.de/umwelt/23469846_Frankreichs-Justiz-ermittelt-wegen-Plastikgranulats-an-der-Atlantikkueste.html (accessed on 8 January 2024).
41. Breilh, J.F.; Bertin, X.; Chaumillon, É.; Giloy, N.; Sauzeau, T. How frequent is storm-induced flooding in the central part of the Bay of Biscay? *Glob. Planet. Chang.* **2014**, *122*, 161–175. [CrossRef]
42. Story, R. Folium—Make Beautiful Maps with Leaflet.js & Python. Available online: https://python-visualization.github.io/folium/latest/ (accessed on 20 January 2024).
43. Sievers, J. Entwicklung und Anwendung Eines Datenbasierten Multikomponenten-KüStenevolutionsmodells am Beispiel der Deutschen NordseeküSte. Ph.D. Thesis, Gottfried Wilhelm Leibniz Universität Hannover, Hannover, Germany, 2022. [CrossRef]
44. Rahman, S.M.A.; Robin, G.S.; Momotaj, M.; Uddin, J.; Siddique, M.A.M. Occurrence and spatial distribution of microplastics in beach sediments of Cox's Bazar, Bangladesh. *Mar. Pollut. Bull.* **2020**, *160*, 111587. [CrossRef] [PubMed]
45. Eberhardt, L.L. Transect Methods for Population Studies. *J. Wildl. Manag.* **1978**, *42*, 1–31. [CrossRef]
46. Fanini, L.; Bozzeda, F. Dynamics of plastic resin pellets deposition on a microtidal sandy beach: Informative variables and potential integration into sandy beach studies. *Ecol. Indic.* **2018**, *89*, 309–316. [CrossRef]
47. Microsoft Corporation. Microsoft Excel. Available online: https://office.microsoft.com/excel (accessed on 20 January 2024).
48. Inkscape Project. Inkscape. Available online: https://inkscape.org (accessed on 20 January 2024).
49. Van Rossum, G.; Drake, F.L. *Python 3 Reference Manual*; CreateSpace: Scotts Valley, CA, USA, 2009.
50. Pandas Development Team. *pandas-dev/pandas: Pandas*; Zenodo: Genève, Switzerland, 2020. [CrossRef]
51. Wes McKinney. Data Structures for Statistical Computing in Python. In Proceedings of the 9th Python in Science Conference (SciPy 2010), Austin, TX, USA, 28 June–3 July 2010; pp. 56–61. [CrossRef]
52. Gazoni, E.; Clark, C. Openpyxl—A Python Library to Read/Write Excel 2010 xlsx/xlsm Files. 2023. Available online: https://openpyxl.readthedocs.io/en/stable/ (accessed on 20 January 2024).
53. Barker, C. lat_lon_parser-simple Parser for Latitude-Longitude Strings. 2022. Available online: https://pypi.org/project/lat-lon-parser/ (accessed on 20 January 2024).
54. Hunter, J.D. Matplotlib: A 2D graphics environment. *Comput. Sci. Eng.* **2007**, *9*, 90–95. [CrossRef]
55. Kamalov, F. Kernel density estimation based sampling for imbalanced class distribution. *Inf. Sci.* **2020**, *512*, 1192–1201. [CrossRef]
56. Hintze, J.L.; Nelson, R.D. Violin Plots: A Box Plot-Density Trace Synergism. *Am. Stat.* **1998**, *52*, 181–184. [CrossRef]
57. Tanious, R.; Manolov, R. Violin Plots as Visual Tools in the Meta-Analysis of Single-Case Experimental Designs. *Methodol. Eur. J. Res. Methods Behav. Soc. Sci.* **2022**, *18*, 221–238. [CrossRef]
58. Aberasturi, D., Violin Plot. In *Wiley StatsRef: Statistics Reference Online*; Wiley: Hoboken, NJ, USA, 2023; pp. 1–7. [CrossRef]
59. Verma, A. *Evaluation of Sea Sand and River Sand Properties and Their Comparison*; National Dong Hwa University: Hualien, Taiwan, 2015. [CrossRef]
60. Salles, P.; Valle-Levinson, A.; Sottolichio, A.; Senechal, N. Wind-driven modifications to the residual circulation in an ebb-tidal delta: Arcachon Lagoon, Southwestern France. *J. Geophys. Res. Ocean.* **2015**, *120*, 728–740. [CrossRef]
61. Azaaouaj, S.; Nachite, D.; Anfuso, G.; Er-Ramy, N. Abundance and distribution of microplastics on sandy beaches of the eastern Moroccan Mediterranean coast. *Mar. Pollut. Bull.* **2024**, *200*, 116144. [CrossRef] [PubMed]
62. Masud, A.; Gül, M.; Küçükuysal, C.; Buluş, E.; Şahin, Y.M. Effect of lithological properties of beach sediments on plastic pollution in Bodrum Peninsula (SW Türkiye). *Mar. Pollut. Bull.* **2023**, *190*, 114895. [CrossRef] [PubMed]
63. Blair, R.; Waldron, S.; Phoenix, V.; Gauchotte-Lindsay, C. Microscopy and elemental analysis characterisation of microplastics in sediment of a freshwater urban river in Scotland, UK. *Environ. Sci. Pollut. Res.* **2019**, *26*, 12491–12504. [CrossRef] [PubMed]
64. Schröder, K.; Kossel, E.; Lenz, M. Microplastic abundance in beach sediments of the Kiel Fjord, Western Baltic Sea. *Environ. Sci. Pollut. Res.* **2021**, *28*, 26515–26528 [CrossRef] [PubMed]
65. Stolte, A.; Forster, S.; Gerdts, G.; Schubert, H. Microplastic concentrations in beach sediments along the German Baltic coast. *Mar. Pollut. Bull.* **2015**, *99*, 216–229. [CrossRef] [PubMed]
66. Hayes, A.; Kirkbride, K.P.; Leterme, S.C. Variation in polymer types and abundance of microplastics from two rivers and beaches in Adelaide, South Australia. *Mar. Pollut. Bull.* **2021**, *172*, 112842. [CrossRef] [PubMed]
67. Sbarberi, R.; Magni, S.; Boggero, A.; Della Torre, C.; Nigro, L.; Binelli, A. Comparison of plastic pollution between waters and sediments in four Po River tributaries (Northern Italy). *Sci. Total. Environ.* **2024**, *912*, 168884. [CrossRef] [PubMed]

68. Ioanna, T.; Amalia, M. Microplastic Particles in Sandy Beaches of Thessaloniki Gulf, Greece. *WSEAS Trans. Environ. Dev.* **2023**, *19*, 1380–1385. [CrossRef]
69. Acosta Coley, I.; Olivero-Verbel, J. Microplastic resin pellets on an urban tropical beach in Colombia. *Environ. Monit. Assess.* **2015**, *187*, 4602. [CrossRef]
70. OSPAR Commission. *Third Integrated Report and Assessment on the Eutrophication Status of the OSPAR Maritime Area under the Common Procedure*; OSPAR Commission: London, UK, 2017.
71. Kalogerakis, N.; Karkanorachaki, K.; Kalogerakis, G.C.; Triantafyllidi, E.I.; Gotsis, A.D.; Partsinevelos, P.; Fava, F. Microplastics Generation: Onset of Fragmentation of Polyethylene Films in Marine Environment Mesocosms. *Front. Mar. Sci.* **2017**, *4*, 84. [CrossRef]
72. Marti, E.; Martin, C.; Galli, M.; Echevarría, F.; Duarte, C.M.; Cózar, A. The Colors of the Ocean Plastics. *Environ. Sci. Technol.* **2020**, *54*, 6594–6601. [CrossRef] [PubMed]
73. Enders, K.; Lenz, R.; Stedmon, C.A.; Nielsen, T.G. Abundance, size and polymer composition of marine microplastics $\geq$ 10 µm in the Atlantic Ocean and their modelled vertical distribution. *Mar. Pollut. Bull.* **2015**, *100*, 70–81. [CrossRef] [PubMed]
74. Becker, W.; Sachsenheimer, K.; Klemenz, M. Detection of Black Plastics in the Middle Infrared Spectrum (MIR) Using Photon Up-Conversion Technique for Polymer Recycling Purposes. *Polymers* **2017**, *9*, 435. [CrossRef] [PubMed]
75. Phuong, N.N.; Poirier, L.; Pham, Q.T.; Lagarde, F.; Zalouk-Vergnoux, A. Factors influencing the microplastic contamination of bivalves from the French Atlantic coast: Location, season and/or mode of life? *Mar. Pollut. Bull.* **2018**, *129*, 664–674. [CrossRef] [PubMed]
76. Plages des Landes. Metro Beach: Landes Beaches. 2023. Available online: http://www.plages-landes.info/en/tarnos-en/plage-du-metro-2/ (accessed on 10 January 2024).
77. Majewsky, M.; Bitter, H.; Eiche, E.; Horn, H. Determination of microplastic polyethylene (PE) and polypropylene (PP) in environmental samples using thermal analysis (TGA-DSC). *Sci. Total. Environ.* **2016**, *568*, 507–511. [CrossRef] [PubMed]